Communications in Physics, Vol. 22, No. 2 (2012), pp. 147-153

A STUDY OF THE OPTICAL PROPERTIES OF Sm-DOPED $ZnWO_4$ SYNTHESIZED BY HYDROTHERMAL METHOD

NGUYEN MANH HUNG
Center for Nano Science and Technology and Department of Physics, Hanoi National University of Education
and
Hanoi University of Mining and Geology
NGUYEN MANH AN
Hong Duc University
NGUYEN VAN MINH
Center for Nano Science and Technology and Department of Physics, Hanoi National University of Education

Abstract. *The $ZnWO_4$:Sm^{3+} compounds were prepared by hydrothermal method and characterized by X-ray diffraction (XRD), scanning electron microscopy (SEM), Raman scattering, absorption and photoluminescent (PL) techniques. This rare earth material presents high orange luminescence intensity under UV radiation. The excitation spectra of the compound presented broad bands arising from ligand-to-metal charge transfer (LMCT) (O→W and O→Sm^{3+}) and narrow bands from 4f-intraconfigurational transitions. The emission spectra exhibited the $^4G_{5/2} \rightarrow {}^6H_J$ (J = 5/2, 7/2, 9/2 and 11/2) transition (direct excitation), for the system doped with Sm^{3+}, while the broad band assigned to the LMCT (O→W) is observed when the excitation is monitored on the O→W LMCT state around 270 nm.*

I. INTRODUCTION

Zinc tungstate ($ZnWO_4$) with a wolframite structure has been of practical interest for a long time because of its attractive luminescence [1]. $ZnWO_4$ has been applied as a possible new material for microwave amplification by stimulated emission of radiation [2], scintillator [3] and optical hole burning lattice material [4], etc. Recently, new applications for this material have emerged, including large-volume scintillators for high-energy physics [5]. Besides that, the excited tungstate group may effectively transfer energy to rare earths. In the past few years, there have been many papers concerned with the preparation and photoluminescence properties of rare earth-doped tungstates crystals [6,7]. In these, the trivalent samarium can generate red emissions in some tungstate crystals [7,8], that may make the tungstates emit blue-green light and become a potential white-light phosphor. However, Sm-doped tungstates in the forms of powder and film, especially Sm-doped $ZnWO_4$ material, have not been reported for the luminescence application.

$ZnWO_4$ has been prepared by different routes such as the Czochralski method [9], reaction in aqueous solution followed by heating of the precipitate [10], sol-gel reaction

[11], and hydrothermal reaction over an extensive period [12]. However, $ZnWO_4$ particles prepared by these routes are relatively large in particle size and irregular in morphology. One of the new routes to prepare $ZnWO_4$ with nanometer size is hydrothermal method. Although a few studies on the chemical synthesis of zinc tungstate by the hydrothermal method have been reported, very few papers were concerned with effects of the size and morphology and Sm dopant on the optical properties of $ZnWO_4$ nanoparticles.

In this work, we report the synthesis of Sm doped $ZnWO_4$ nanopowder by hydrothermal method at a low temperature of 180°C and investigate their structure, Raman scattering, absorption and photoluminescence.

II. EXPERIMENT

Zinc tungstate ($ZnWO_4$) nanoparticles were prepared by the hydrothermal reaction of $Zn(NO_3)_2.6H_2O$, $Na_2WO_4.2H_2O$ and $Sm(NO_3)_3$ at temperature of 180°C for 8 h. In a typical procedure for the preparation of sample, $Zn(NO_3)_2.6H_2O$ (1 mmol) in water (10 ml) was added $Na_2WO_4.2H_2O$ (1 mmol) and $Sm(NO_3)_3$ in water (20 ml) with vigorous stirring. H_2O was added to make 40 ml of the solution, and pH of the solution was adjusted to 6.68, respectively, with dilute of 30% $NH_3.H_2O$ solution. The solution was then added into a Teflon-lined stainless steel autoclave of 100 ml capacity. The autoclave was heated to 180°C for 8 h without shaking or stirring. Afterwards, the autoclave was allowed to cool to room temperature gradually. The white precipitate collected was washed with distilled water four times. The solid was then heated at 80°C and dried under vacuum for 2.5 h.

Structural characterization was performed by means of X-ray diffraction using a D5005 diffractometer with Cu Kα radiation. The FE-SEM observation was carried out by using a S4800 (Hitachi) microscope. Raman measurements were performed in a back scattering geometry using Jobin Yvon T 64000 triple spectrometer equipped with a cryogenic charge-coupled device (CCD) array detector, and the 514.5 nm line of Ar ion laser. The absorption spectra were recorded by using Jasco 670 UV-vis spectrometer and the room temperature luminescent spectra were recorded on a spectrofluorometer (PL, Fluorolog-3, Jobin Yvon Inc, USA).

III. RESULT AND DISCUSSION

Fig. 1 shows the XRD patterns of Sm doped $ZnWO_4$ powders heated for 8 h. It is noted that the $ZnWO_4$ single phase could be observed in all XRD patterns. All diffraction peaks of $ZnWO_4$ crystal appeared when the sample was prepared at 180°C, which could be easily indexed as a pure, monoclinic wolframite tungstate structure according to the standard card (JCPDS Card number: 73-0554), except the peak at $2\theta = 27^0$ for sample with $x \geq 0.05$. It was found that, the optimum temperature for the production of the high-quality crystal was as high as 180°C [13].

The SEM micrographs of the ZnWO4 and Sm-doped ZnWO4 powders are shown in Fig. 2, which indicates that the average particle size was about 200–500 nm for the $ZnWO_4$ powders and about 150–400 nm for the Sm-doped powders. It is clear that the size was decreased by the Sm substitution. This could be due to the inhibition in the crystalline growth of the powders produced by the Sm substitution. It is generally believed that this

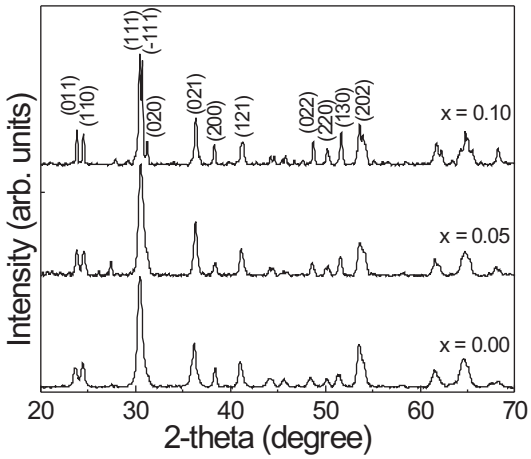

Fig. 1. XRD patterns of Sm doped $ZnWO_4$with x = 0.00 and 0.05

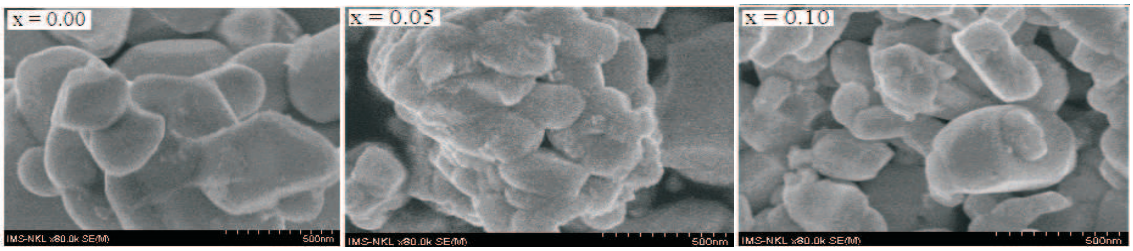

Fig. 2. SEM images of Sm doped $ZnWO_4$ nanopowders

inhibition is associated with the crystal lattice distortion resulting from the larger ionic radius of Sm^{3+} (1.04 Å) compared with Zn^{2+} (0.74 Å).

Fig. 3 shows a diffuse reflection spectrum of Sm doped $ZnWO_4$ nanopowder. Steep shape of the spectra indicated that the UV light absorption was due to the band-gap transition instead of the transition from the impurity level. For a crystalline semiconductor, the optical absorption near the band edge follows the equation: $ah\nu = A(h\nu - E_g)^{1/n}$, where a, ν, E_g, and A are absorption coefficient, light frequency, band gap, and a constant, respectively [14]. For the $ZnWO_4$, n is determined to be 2. Thus, the band gaps of the Sm doped $ZnWO_4$ nanopowders were roughly estimated to be 3.74, 3.76 and 3.79, as shown in the inset of Fig. 3. Bonanni et al. [15] reported that the band gap of $ZnWO_4$ was 3.75 eV, which is in agreement to our experimental values. More further, in the spectra of Sm doped powders appears an absorption peak around 405 nm. This would originate from Sm dopant.

Fig. 4 illustrates the Raman spectra for Sm doped $ZnWO_4$ nanopowdes. It is clear that, the peak shifts to higher frequency as increasing the Sm content. Studies of the optical properties and the Raman spectra of $ZnWO_4$ at room temperature have been

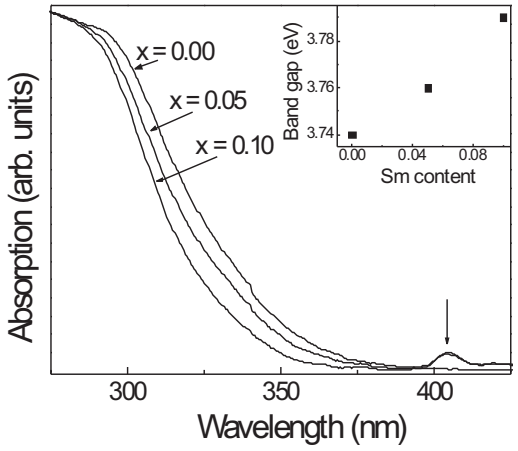

Fig. 3. Absorption spectra of Sm doped $ZnWO_4$ nanopowders

reported in the literature [16]. $ZnWO_4$ has the monoclinic wolframite structure with C_{2h} point group symmetry and P2/c space group. It has two formula units per unit cell. The W-O interatomic distance is substantially smaller than that of Zn-O, therefore, to a first order approximation, the lattices can be separated into internal vibrations of the octahedra and the external vibrations in which an octahedron vibrates as a unit. A group theoretical calculation of the $ZnWO_4$ structure yields 36 lattices modes, of which 18 are Raman active ($8A_g + 10B_g$).

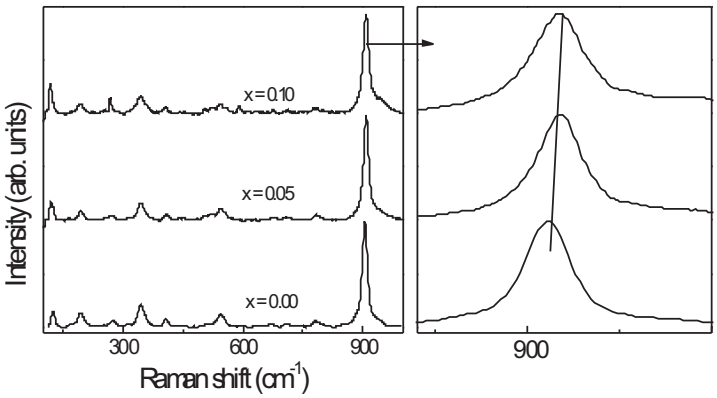

Fig. 4. Raman spectra of Sm doped $ZnWO_4$ nanopowders. The right one is the enlarged peak of 900 cm^{-1}.

It is assigned to the A_g mode observed near 907 cm^{-1} since, as in the case of the regular octahedron, the symmetric stretch is expected to have the highest frequency of all the internal modes. The E_g mode (asymmetric stretch) of the regular octahedron splits into $A_g + B_g$ by the crystal field. Again, these modes are expected to have frequencies

that are higher than those of the bending mode (T_{2g}) of the regular octahedron. The obvious choices are the B_g and A_g modes observed near 786 and 709 cm^{-1}, respectively. The remaining modes $2A_g + B_g$ with frequencies of 407, 342 and 190 cm^{-1} are assigned to the T_{2g} mode of the regular octahedron.

In a first attempt to identify the six internal stretching modes of the W-O atoms in the distorted WO_6 octahedra of $ZnWO_4$, Liu et al. [17] assigned them to the modes at 906, 787 and 407 cm^{-1} on the basis of the bond lengths and Raman frequencies in the WO_6 group. Afterwards, Wang et al. [18] assigned the internal stretching modes to the phonons observed near 906, 787, 709, 407, 342, and 190 cm^{-1} on the basis of the temperature dependence of the Raman frequencies. However, this assignment is in contradiction with the fact that the frequencies of the internal modes are expected to be higher than those of the external modes. These authors argue in favor of their assignment that the oxygen sharing between WO_6 and ZnO_6 octahedra may cause a considerable overlap in the frequency range for the two types of vibrations. For the Sm doped powders, the peak shifts to higher wavenumber as increasing the Sm content and some new peaks appear around 600 cm^{-1}. This suggets the solubility of the Sm, although it can not be observed in XRD result.

Fig. 5a shows the representative PL spectra of the $ZnWO_4$ crystallites synthesized by the hydrothermal method for 8 h. With the exited wavelength at 324 nm, the corresponding emission peaks centered at $\sim$ 500 nm can be observed. This broad emission band had a shoulder in the blue region, indicating it consisted of more than one emission band. The PL spectra were fit to three peaks using a Gauss function as shown in Fig. 5a.

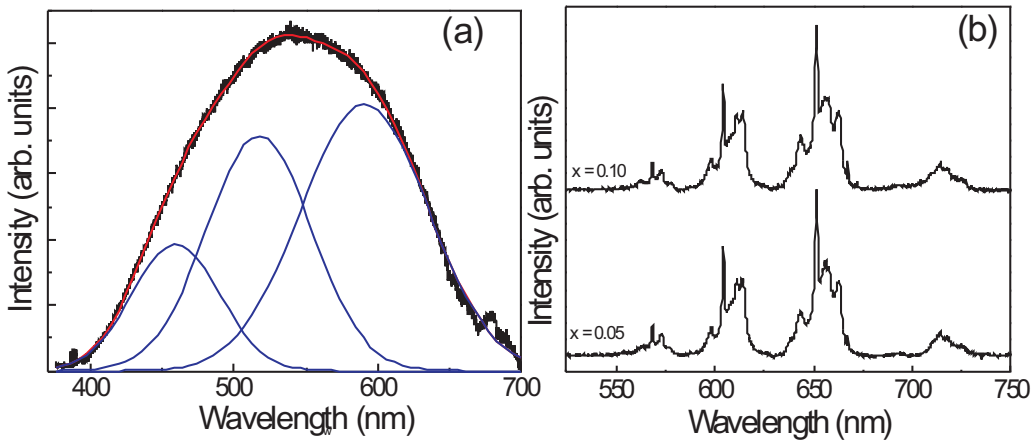

Fig. 5. (a) PL spectra of the $ZnWO_4$ synthesized by the hydro thermal method for 8 h (the solid lines are fitting results by using Gauss distribution); (b) Emission spectra of the Sm^{3+} doped $ZnWO_4$ at room temperature

It is well established that the W_6^{6-}complex and a slight deviation from perfect order in the crystal structure are responsible for the emission bands [19]. But there exist different opinions concerning the origin of these bands. Lammers [20] and Grigorjeva [21] believed

that the blue and green emissions originated from the intrinsic W_6^{6-} complex with a double emission from one and the same center ($^3T_{1u} \rightarrow {}^1A_{1g}$), whereas the yellow emission is due to recombination of e–h pairs localized at oxygen atom deficient tungstate ions. However, Ovechkin [22] ascribed the blue band to the self-trapped exciton in tungstenite crystals with strong electron–phonon coupling, and the green and yellow bands to the transitions of $T_{2u} \rightarrow T_{2g}$ and $T_{1g} \rightarrow T_{2g}$ in the W_6^{6-} complex. Almost all investigations in luminescent properties of $ZnWO_4$ have been carried out for large crystals and films. The nanosized $ZnWO_4$ prepared via a hydrothermal route in the current work showed luminescent properties similar to those of bulk $ZnWO_4$. Further studies on PL property of the as-prepared $ZnWO_4$ crystallites are in progress.

The emission spectra of the Sm^{3+}-doped compounds at room temperature, in the range of 500-750 nm were shown in Fig. 5b. The samples doped with Sm showed an emission typical of samarium ions. These spectra show only the bands due to 4f-4f transitions arising from the $^4G_{5/2}$ emitting level. The relatively high intensity bands are those arising from the $^4G_{5/2}.\rightarrow {}^6H_J$ transitions (where J = 5/2, 7/2, 9/2 and 11/2), which are split in the maximum number of (J+1/2) components, indicating that the Sm^{3+} ion occupies a site with low symmetry. It is also observed that the forced electric dipole $^4G_{5/2}.\rightarrow {}^6H_{9/2}$ transition presents the highest relative emission intensity at 643 nm.

IV. CONCLUSIONS

In conclusion, Sm doped $ZnWO_4$ nano-particles were successfully synthesized at 180°C by a hydrothermal route. The morphology and dimension of the $ZnWO_4$ crystallites were affected by Sm doping.

The grain size of the powders was decreased with increasing Sm content. The powders showed a broad excitation band and a broad deep blue-green emission band. The Sm substitution resulted in emissions at 568, 603 and 642 nm.

ACKNOWLEDGMENTS

This work was supported by the National Foundation for Science and Technology Development (NAFOSTED) of Vietnam and the Research Foundation – Flanders (FWO) of Belgium (Code FWO.2011.23).

REFERENCES

[1] F.A. Kröger, *Some Aspects of the Luminescence of Solids*, Elsevier, Amsterdam, 1948.
[2] L.G. Van Uitert, S. Preziosi, *J. Appl. Phys.* **33** (1962) 2908.
[3] P. F. Schofield, K. S. Knight, G. Cressey, *J. Mater. Sci.* **31** (1996) 2873.
[4] A. Caprez, P. Meyer, P. Mikhail, *J. Hulliger, Mater. Res. Bull.* **32** (8) (1997) 1045.
[5] N. Klassen, S. Shmurak, B. Red'kin, B. Ille, B. Lebeau, P. Lecoq, and M. Schneegans, *Nucl. Instrum. Methods Phys. Res.* **A486**, (2002) 431.
[6] Fugui Yang, Chaoyang Tu, Hongyan Wang, Yanping Wei, Zhenyu You, Guohua Jia, Jianfu Li, Zhaojie Zhu, Xiuai Lu, and Yan Wang, *J. Alloys Compd.* **455** (2008) 269–273.
[7] M. Treadaway and R. Powell, *Phys. Rev.* **B11** (1975) 862–874.
[8] G. Born, A. Hofstaetter, A. Scharmann, and G. Schwarz, *J. Lumin.* **1/2** (1970) 641–650.
[9] J.C. Brice, P.A.C. Whiffin, Br. *J. Appl. Phys.* **18** (1967) 581.
[10] A. Kuzmin, J. Purans, *Radiat. Meas.* **33** (2001) 583.

[11] M. Bonanni, L. Spanhel, M. Lerch, E. Fuglein, G. Muller, *Chem. Mater.* **10** (1998) 304.
[12] F.-S. Wen, X. Zhao, H. Huo, J.-S. Chen, E.-S. Lin, J.-H. Zhang, *Mater. Lett.* **55** (2002) 152.
[13] H. Fu, J. Lin, L. Zhang, Y. Zhu, *Applied Catalysis A: General* **306** (2006) 58–67.
[14] M.A. Butler, *Appl. Phys.* **48** (1977) 1914.
[15] M. Bonanni, L. Spanhel, M. Lerch, E. Fuglein, G. Muller, *Chem. Mater.* **10** (1998) 304.
[16] H. Wang, Y. Liu, I. D. Zhou, G. Chen, T. Zhou, J. H. Wang and B. Q. Hu, *Acta Phys. Sin.* **38** (1989) 670.
[17] Y. Liu, H. Wang, G. Chen, Y. D. Zhou, B.Y. Gu and B. Q. Hu, *J. Appl. Phys.* **64** (1988) 4651.
[18] H. Wang, F. D. Medina, Y. D. Zhou, and Q. N. Zhang, *Phys. Rev.* **B45** (1992) 10356.
[19] G. Blasse, Structure and Bonding 42, Springer, Berlin,1980.; M.J.J. Lammers, G. Blasse, D. S. Robertson, *Phys. Status Solidi* **A63** (1981) 569.
[20] M.J.J. Lammers, G. Blasse, D. S. Robertson, *Phys. Status Solidi* **A63** (1981) 569.
[21] L. Grigorjeva, R. Deych, D. Millers, S. Chernov, *Radiat. Meas.* 29 (3–4) (1998) 267.
[22] A. E. Ovechkin, V. D. Ryzhikov, *et al., Phys. Status Solidi* **A103** (1987) 285.

Received 11 November 2011.